Green and Sustainable Environments

Green and Sustainable Environments **1** (2026) 09
https://doi.org/10.62755/gsenv.2026.09
journal homepage: pubs.greensus.org/gsenv

Check for updates



RESEARCH PAPERS

# Field Calibration of Low-Cost SHT20 and BH1750 Sensors for Microclimate Monitoring in a Tropical Greenhouse: Effects of Calibration Range and Transmission Interval

Zunanik Mufidah[1,*], Mahardika Priya Tumanggor[1], Kisna Pertiwi[1]

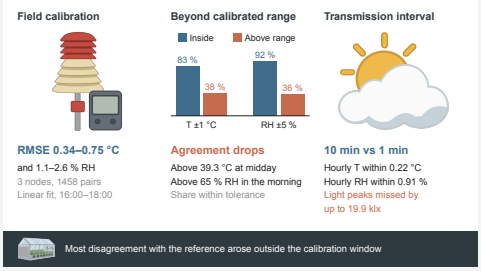
[1] *Department of Biosystems Engineering, Faculty of Industrial Technology, Institut Teknologi Sumatera, Terusan Ryacudu, Way Hui, Jati Agung, Lampung Selatan 35365, Indonesia*

∗ **Corresponding author**: zunanik.mufidah@tbs.itera.ac.id

**ARTICLE HISTORY**: Received: September 23, 2026 · Revised: November 17, 2026 · Accepted: November 17, 2026

## ABSTRACT

Low-cost sensor nodes now drive climate control in many tropical greenhouses, yet their accuracy is usually taken from datasheets rather than tested across the conditions in which a controller acts. Here, three ESP32 nodes with SHT20 temperature and relative humidity (RH) sensors and BH1750 light sensors were calibrated and validated against reference instruments in a fan-and-pad cooled greenhouse in Indonesia and followed through 1458 paired readings per quantity at three times of day. The effect of the transmission interval was isolated by subsampling 1 min series at 5 and 10 min, which holds the weather constant between intervals. Before correction the sensors read up to 2.4 °C warm and 8.5 % RH wet, and a linear correction fitted on a two-hour late-afternoon window brought the validation root-mean-square error (RMSE) to 0.34–0.75 °C and 1.1–2.6 % RH, within the stated accuracy of reference instruments that are not traceable; these figures measure agreement with that reference, not absolute accuracy. In the field, 83 % of temperature readings agreed with the reference to within ±1 °C inside the calibrated range but 38 % above 39.3 °C, mostly at midday, and the share of humidity readings within ±5 % RH fell from 92 % to 36 % above 65 % RH in the morning. In 18 hourly windows, a 10 min interval changed hourly means of temperature and humidity by no more than 0.22 °C and 0.91 % RH, but missed hourly illuminance peaks by up to 19.9 klx under rapidly varying light. In this greenhouse, most of the disagreement with the reference arose outside the calibration window, which suggests, though this was not tested, that field calibrations of low-cost nodes should span the midday heat and the morning humidity at which cooling decisions are made.




**KEYWORDS** *greenhouse microclimate; low-cost sensors; field calibration; evaporative cooling; transmission interval; humid tropics*

## 1. INTRODUCTION

Protected cultivation is expanding in hot and humid regions, where greenhouses shelter crops from heavy rain and insects but trap heat [1, 2]. Without active cooling the air in such a house can pass 47 °C and stay above 70 % relative humidity on most days [3], and tomato grown under net screens in the Malaysian lowlands has been exposed to 39.7 °C and 98.9 % relative humidity [4]. Fan-and-pad evaporative cooling is the usual remedy, and it is a resource cost as well as a climate control: in one fan-and-pad house the pads used 8.4 to 14 L of water and the fans 48 to 100 W h of electricity per square metre of floor each day, and both rise with the hours the controller keeps them running [5, 6]. That controller acts on what its sensors report. A temperature sensor that reads 2 °C high would keep the fans and pads running longer than the crop requires, and a humidity sensor that reads 5 % relative humidity too high would shift every humidity-based decision by the same amount, so the quality of the measurement bears directly on the water and energy the house uses.

Low-cost sensor nodes have made dense monitoring of greenhouse climate affordable. A microcontroller such as the ESP32 with digital temperature, humidity and light sensors costs a small fraction of a research-grade station and can publish readings over Wi-Fi to cloud dashboards at intervals of a minute or less [7–9]. Their accuracy in the field, however, is usually taken from the manufacturer's datasheet or from a short comparison on the bench, and few low-cost temperature sensors have been calibrated in the field [10], and evaluations in the field have found significant humidity bias even where the correlation with the reference was high [11]. Neither study describes a greenhouse. Unshielded sensors warm in sunlight and read high [12–14], capacitive humidity elements drift, most at high humidity [15, 16], and inexpensive light sensors saturate in direct sun [17, 18]. Evaluations against reference instruments have shown that a linear correction removes much of the offset of such sensors [19, 20].

Two questions about these corrections are rarely asked. The first is whether a correction holds outside the conditions it was fitted on. Calibrations of low-cost sensors are most often made indoors, and the range they cover changes their outcome [10]. The air in a tropical greenhouse, by contrast, spanned 28–48 °C and 19–82 % relative humidity over the test days of this study (Section 3.4), so a controller can spend much of its time in conditions the calibration never saw. The second concerns the transmission interval, which is usually chosen for battery life, bandwidth or storage. Observation guidance treats a 1 min average as most suitable and accepts up to 10 min [21], but whether a 10 min series carries the same information for control as a 1 min series depends on how fast each quantity changes, and light under broken cloud changes within seconds [22]. Comparing intervals recorded on different days, moreover, mixes the effect of the interval with that of the weather.

Herein, we calibrated and validated three low-cost nodes (ESP32 with SHT20 and BH1750 sensors) against reference instruments in a fan-and-pad cooled greenhouse in Lampung, Indonesia, and followed them through 1458 paired readings per quantity at three times of day. We asked whether the corrected sensors agree with the reference within its stated accuracy, whether that agreement depends on the range covered by the calibration, and, by subsampling the 1 min series, how much information a 5 or 10 min interval loses. The greenhouse is one example of a class of settings, evaporatively cooled houses in the humid tropics monitored with low-cost nodes. In this house we measured how, and by how much, a short field calibration fails across a wide diurnal range. The results bear on two questions that other houses can test: how wide a calibration window must be, and which quantities tolerate a sparse transmission interval.



e-ISSN 3124-4610 · © 2026 The Authors · CC BY 4.0 OPEN ACCESS

## 2. MATERIALS AND METHODS

### 2.1 Greenhouse and Measurement Points

Measurements were made from March to June 2024 in the arch-type research greenhouse, covered with translucent plastic, on the campus of Institut Teknologi Sumatera (ITERA), Lampung Selatan, Indonesia (5.37° S, 105.31° E); its floor dimensions were not recorded. The greenhouse is cooled by an evaporative pad at one end and exhaust fans at the other; whether the pad and fans ran during each measurement was not recorded. Three identical sensor nodes were placed along the long axis of the house (Fig. 1a): point 1 near the cooling pad, point 2 at the centre, and point 3 near the exhaust fans, at 2.7, 12.7, and 22.06 m from the pad end and 4.1 m from the side wall. Each node was mounted on a vertical pole with its sensors about 1.5 m above the floor and the light sensor facing upwards (Fig. 1c).

### 2.2 Monitoring System

Each node consisted of an ESP32 microcontroller (NodeMCU), an SHT20 digital sensor for air temperature and relative humidity (RH), and a GY-30 module carrying a BH1750 ambient-light sensor (Table 1). Both sensors shared the $I^2C$ bus of the ESP32 (SDA on GPIO 21, SCL on GPIO 22) and were powered at 3.3 V. The sensors and the ESP32 were fixed to one foam disc (Fig. 1b), and the disc was mounted under a conical cover with a louvred cap (Fig. 1c), which shaded the electronics from direct sun but was not ventilated by a fan; the sensor therefore exchanged heat with the air only by natural convection, and it shared that enclosed space with the ESP32. Three time scales are involved in each transmitted value and are kept apart here: the conversion time of the sensors, below 0.1 s for the SHT20 [16] and about 0.12 s for the BH1750 in its high-resolution mode [17]; the rate at which the firmware read the sensors; and the transmission interval of 1, 5 or 10 min. The firmware transmitted a single instantaneous reading taken at transmission time, not an average of readings taken between transmissions; the BH1750 measurement time actually set was not recorded. Readings were published over Wi-Fi to an MQTT broker, passed through a REST interface to a cloud server, and displayed with their timestamps in the ITERAHERO web application. The transmission interval was set in firmware to 1, 5, and 10 min in the respective performance tests (Section 2.5).

### 2.3 Reference Instruments

The reference for air temperature and relative humidity was the HTC-2 thermohygrometer, a generic hand-held instrument without a manufacturer's datasheet or calibration certificate, and that for illuminance the UNI-T UT383 luxmeter (Table 1). Because neither instrument carried a calibration traceable to a standard, all results in this paper describe agreement with these reference instruments, not traceable measurement accuracy. To size the uncertainty this leaves, the stated accuracy of each instrument was treated as the half-width of a rectangular distribution and combined with its display resolution. For the HTC-2 this gives standard uncertainties of 0.58 °C and 2.9 % RH (expanded, $k = 2$: 1.2 °C and 5.8 % RH); for the UT383 it gives an expanded uncertainty of 6.0–6.7 % of the reading at the median illuminances within and above the calibrated range in the performance tests (12.2 and 47.1 klx). A random reference error of this size inflates the root-mean-square error (RMSE) between sensor and reference, and a systematic one shifts the bias by up to the stated accuracy, so differences smaller than the stated accuracy cannot be attributed to the sensor. The tightest stated accuracies of the HTC-2, ±1 °C and ±5 % RH, were therefore used as the agreement criterion; they are looser than the typical accuracy of the SHT20, so the comparison bounds the error of the corrected sensors from above rather than resolving it. The reference instruments were placed beside the sensor node, at a distance and height that were not recorded, and their displays were recorded by camera (Fig. 1c), so that each reference reading could be paired with the sensor reading carrying the same timestamp.

### 2.4 Calibration and Validation

At each point, sensor and reference readings were paired every minute from 16:00 to 18:00 local time (UTC + 7), giving 121 pairs per quantity and point. The calibration therefore covered the conditions of a single late-afternoon window: reference values of 31.3–39.3 °C, 41–65 % RH and 4.1–35.4 klx across the three points. The window was chosen because in the late afternoon all three quantities change slowly and in one direction, temperature and illuminance falling and relative humidity rising, so that one session spans a range of each, and because the readings are less disturbed by direct sun and passing cloud than at midday; only this window was used. Calibration and validation were carried out on different days, whose dates were not recorded; the validation day was warmer (reference up to 43.7 °C) and spanned 34–69 % RH, so the two data sets did not share the same conditions. The calibration data of each quantity and point were fitted by ordinary least squares as

$$s = a\,r + b, \tag{1}$$

where $s$ is the raw (uncorrected) sensor reading, $r$ the reference reading, and $a$ and $b$ the fitted slope and intercept. Each raw reading was then corrected by inverting Eq. (1),

$$\hat{r} = \frac{s - b}{a}, \tag{2}$$

where $\hat{r}$ is the corrected reading, the sensor's estimate of the reference value. The coefficients of each point were entered in the firmware of its node, and the validation data were recorded with the correction active, so that the validation pairs compare $\hat{r}$ with $r$. Calibration and validation together comprise 2178 reading pairs (two stages, three quantities, three points, 121 pairs each).

### 2.5 Performance Tests

With the corrected firmware, sensor and reference readings were recorded at the three points in three one-hour windows (07:00–08:00, 12:00–13:00 and 16:00–17:00), at transmission intervals of 1, 5 and 10 min, which yield 61, 13 and 7 readings per window. Each combination of window and interval was repeated on two days. Each interval was run on its own pair of days, so that differences between intervals include day-to-day differences in weather; the dates were not recorded.

Reference readings were taken at the three points in the same minutes, with one set of reference instruments per point. The tests yielded 486 reading pairs per point and quantity (1458 per quantity). The display resolution of the reference instruments is 0.1 °C, 1 % RH, and 1 or 10 lx below and above 10 klx, respectively (Table 1). In 43 of the 162 one-hour windows (54 per quantity: 3 points × 3 windows × 3 intervals × 2 days; 6 for temperature, 22 for relative humidity and 15 for illuminance; in 19 of them all values, in 24 some) the recorded reference values carry a finer resolution than the display, and their origin was not recorded. These values were retained, and every analysis was repeated without the 43 windows (Section 3.2).

Because each interval was run on its own days, the effect of the interval was assessed on the 1 min windows only, by subsampling each 61-reading series at every fifth and every tenth minute (13 and 7 readings). The hourly mean, maximum, minimum and standard deviation of the subsampled series were compared with those of the full series, which holds the weather constant between intervals.

### 2.6 Data Analysis

For $n$ pairs of sensor reading $s_i$ (raw in the calibration, corrected, $\hat{r}_i$, in the validation and performance tests) and reference reading $r_i$, with $d_i = s_i - r_i$, agreement was summarised by the mean bias, the mean absolute error (MAE), the RMSE and the mean absolute percentage error (MAPE), which is most informative for illuminance, whose error grows with the reading:

$$\text{bias} = \frac{1}{n}\sum_{i=1}^{n} d_i, \tag{3}$$

$$\text{MAE} = \frac{1}{n}\sum_{i=1}^{n} |d_i|, \tag{4}$$

$$\text{RMSE} = \left(\frac{1}{n}\sum_{i=1}^{n} d_i^2\right)^{1/2}, \tag{5}$$

$$\text{MAPE} = \frac{100}{n}\sum_{i=1}^{n} \frac{|d_i|}{r_i}. \tag{6}$$

The slope $a$ and intercept $b$ of Eq. (1) describe the response of the sensor relative to the reference, and the coefficient of determination $R^2$ its

© 2026 The Authors | CC-BY 4.0

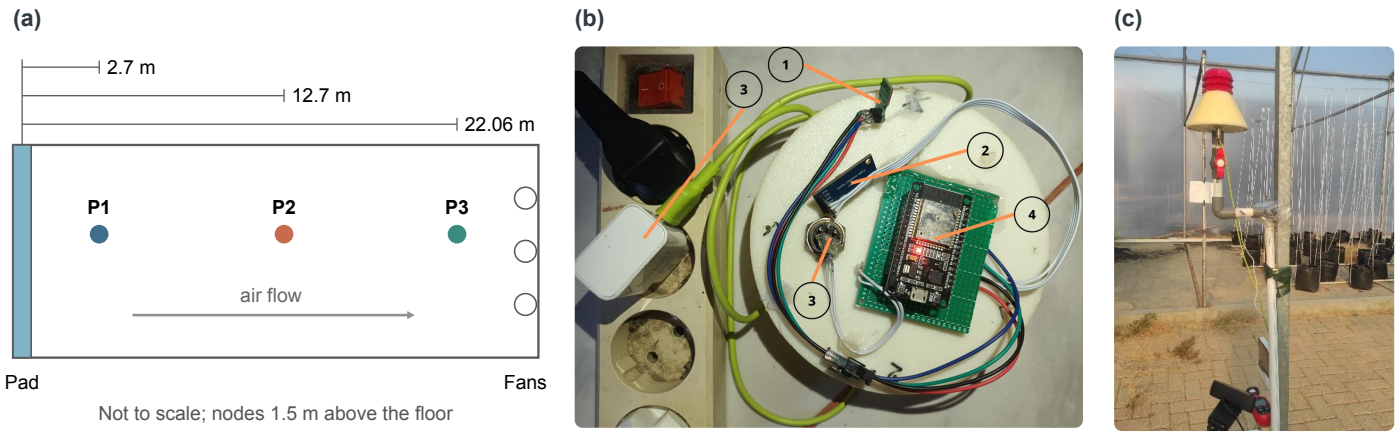



**Figure 1.** Measurement set-up. (a) Plan of the greenhouse with the three measurement points (not to scale). (b) Sensor node: 1, SHT20; 2, GY-30 (BH1750); 3, power supply; 4, ESP32. (c) Node installed under its conical cover.

**Table 1.** Sensors and reference instruments. Specifications as stated by the manufacturers.

| Instrument | Quantity | Range | Stated accuracy |
|---|---|---|---|
| SHT20 | Air temperature | −40 °C to 125 °C | ±0.3 °C typical (5–60 °C) [16] |
| | Relative humidity | 0–100 % | ±3 % RH typical (20–80 % RH) [16] |
| BH1750 (GY-30) | Illuminance | 1–65 535 lx | ±20 % measurement variation [17] |
| HTC-2 thermohygrometer | Air temperature | −10 °C to 50 °C | ±1 °C[a] (resolution 0.1 °C) |
| | Relative humidity | 10–99 % | ±5 % RH[a] (resolution 1 % RH) |
| UNI-T UT383 luxmeter | Illuminance | 0–199 999 lx | ±(4 % of reading + 8 digits) below 10 000 lx, ±(5 % + 10 digits) above (resolution 1 and 10 lx) [23] |

[a] Values adopted in this study; vendor sheets for this generic instrument give 1–2 °C and 5–10 % RH [24].

linearity; for corrected readings the same fit of $\hat{r}$ on $r$ is reported. The metrics were computed for each quantity and point, separately for the calibration data (uncorrected readings), the validation data (corrected readings) and the performance tests. The performance-test readings were further classed by where the reference value lay relative to the range covered by the calibration of that quantity, pooled across the three points (Section 2.4): below it, within it, or above it. Readings outside the range test the corrected equations by extrapolation.

Consecutive one-minute readings are autocorrelated, so their scatter overstates the information they carry. The 95 % confidence intervals (CI) for bias, MAE, RMSE and MAPE were therefore obtained by block bootstrap with 4000 resamples [25]: for the performance tests, whole one-hour windows were resampled (18 per point and quantity), and for the two-hour (121-reading) calibration and validation series, moving blocks of 10 min. The coefficient of determination describes linearity only; a sensor with a constant offset can have $R^2$ close to 1 and still disagree with the reference. Agreement was therefore also examined by Bland–Altman analysis [26]: the mean difference between sensor and reference and the 95 % limits of agreement (mean ± 1.96 standard deviations of the differences), with illuminance differences expressed relative to the mean of each pair because the error of both instruments scales with the reading. A proportional bias was tested as the slope of the difference on the pair mean.

To separate a humidity offset from sensor heating, the uncorrected calibration readings were converted to vapour pressure and dew point with the Magnus approximation [27], and the relative humidity implied by the reference vapour pressure at the sensor's own temperature reading was compared with the sensor's humidity reading.

The agreement criterion was applied at two levels. For a data set, a corrected sensor was taken to agree with the reference when its bias and RMSE fell within the stated accuracy of the reference instrument (Table 1; temperature and humidity only, illuminance being compared by MAPE), since a difference smaller than that accuracy cannot be resolved against the reference. For individual readings, the share whose difference lay within ±1 °C or ±5 % RH was reported for each class relative to the calibrated range (below, within, above); no such share is given for illuminance, whose reference tolerance varies with the reading.

The number of reading pairs entering each stage was: calibration and validation, 121 per point and quantity (363 per quantity in each stage); performance tests, 486 per point and quantity, of which 366, 78 and 42 at the 1, 5 and 10 min intervals (1458 per quantity, 4374 in total); and the subsampling comparison, 18 one-hour windows of the 1 min series per quantity (3 points × 3 windows × 2 days). All calculations were scripted in Python (NumPy, pandas) from the reading pairs, and the coefficients of Eq. (1) agreed with an independent fit in OriginLab to four decimal places.

## 3. RESULTS AND DISCUSSION

### 3.1 Calibration and Validation

Before correction, every SHT20 read warmer and wetter than the reference (Fig. 2a,b; Table 2). The temperature bias was 1.51–2.43 °C across the three points, and the slope of Eq. (1) was 1.34–1.65, so the offset grew with temperature: at point 1 the sensor read 43.8 °C against 38.7 °C at the start of the calibration window, when the house was warmest, and 32.7 °C against 31.4 °C as it cooled. The relative-humidity bias was 5.2–8.5 % RH, above the ±5 % RH accuracy of the reference at all three points. Neither offset was traced to a cause in this design, and the explanations below are candidates. A temperature offset that grows with temperature is what a sensor body warmed above the surrounding air would show: poorly shielded sensors have read 0.8 to 3.0 °C warm in the field, with the bias strongest at the highest temperatures [12], and a Sensirion sensor mounted on the circuit board of a wireless node carried an error that followed solar radiation [20]. Both sources of heat were present here: the SHT20 sat on the same disc as the ESP32, a few centimetres from it, under a cover that shaded it but was not ventilated (Fig. 1b,c). Because the two sources acted together in every reading, and neither solar radiation nor board temperature was measured, their shares cannot be separated, and a contribution of the reference itself cannot be excluded. For the humidity offset one inference does follow from the data. Converted to vapour pressure with the Magnus approximation [27], the uncorrected sensors held 22–27 % more water vapour than the reference (dew point 3.4–4.0 °C higher), whereas a sensor that was only warmer than the air

© 2026 The Authors | CC-BY 4.0

would have read 4.1–6.4 % RH below the reference, because heating biases a capacitive element dry [16, 28]. Heating of the sensor therefore does not explain the humidity offset; the offset lies in the humidity element, in the reference, or in both, and the data cannot decide between them. A drift of the element is one possibility: this sensor is specified to develop a reversible positive offset of 3 % RH after 60 h above 80 % RH [16], and in-service drift of up to 5 % RH has been observed at the high end of the range [15]. A reference error of the same sign is also possible, given an HTC-2 standard uncertainty of 2.9 % RH (Section 2.3). The BH1750 read within about 10 % of the luxmeter without correction (MAPE 8.8–10.6 %), with a slope of 0.95–1.07.

After the correction was applied in firmware, the validation readings fell on the 1:1 line (Fig. 2d–f). The temperature RMSE dropped from 1.73–2.75 °C to 0.34–0.75 °C and the humidity RMSE from 5.3–8.5 % RH to 1.1–2.6 % RH, both inside the accuracy of the reference, while the illuminance MAPE fell from 8.8–10.6 % to 6.0–7.1 %. The validation temperature RMSE is of the same size as the standard uncertainty of the reference, 0.58 °C, and the humidity RMSE is below its 2.9 % RH (Section 2.3). These values therefore show that the corrected sensors agree with the reference to within the resolution of the comparison; they do not establish an accuracy better than ±1 °C or ±5 % RH, because the reference itself is specified no tighter. Bland–Altman limits of agreement for the validation, pooled over the three points, were −0.95 °C to 1.22 °C and −2.5 % to 3.8 % RH. The validation also carried the first sign of the range limit discussed below. The validation day was warmer than the calibration day (reference up to 43.7 °C against 39.3 °C), and above 40 °C the corrected point 2 flattened at 38.5–39.6 °C while the reference read 40.1–41.6 °C (Fig. 2d).

### 3.2 Field Agreement and the Calibrated Range

Over the 486 readings per point of the performance tests, the corrected SHT20 read 0.73 °C warm on average (RMSE 1.16 °C) and the humidity sensor read 1.9 % RH dry (RMSE 3.8 % RH), pooled over the three points (per point in Table 3). Both summaries hide a dependence on where the reading lay relative to the calibrated range. Of the temperature readings, 33 % were above the 39.3 °C ceiling of the calibration, 92 % of them at midday, and 16 % below its 31.3 °C floor, all in the morning (Fig. 3a). Within the calibrated range the mean bias was 0.43 °C (95 % CI 0.22–0.71) and 83 % of readings agreed with the reference to within ±1 °C. Above it the bias rose to 1.19 °C (0.75–1.62) and only 38 % of readings stayed within ±1 °C; below it the bias was 0.75 °C (0.47–0.98) with 76 % within tolerance. The Bland–Altman analysis shows the same asymmetry (Fig. 4a). Within the range the difference did not depend on temperature (slope −0.07, 95 % CI −0.17 to 0.02) and the limits of agreement were −1.05 °C to 1.90 °C; above it the difference grew by 0.21 °C per degree (CI 0.10–0.31) and the upper limit reached 3.3 °C. Inverting Eq. (1) removes a linear slope at any temperature, so a proportional bias that appears only beyond the fitted range is consistent with a sensor–reference relation that steepens above 39.3 °C, which a linear correction fitted below it cannot follow.

Humidity mirrored this on the other side of the day. The calibration window, 16:00–18:00, never saw relative humidity above 65 %, whereas the morning windows reached 82 %. Above 65 % RH the sensor read 5.4 % RH dry on average (95 % CI 3.6–6.8) against 0.8 % RH dry (CI −0.2 to 1.8) within the range, and the share of readings within ±5 % RH fell from 92 % to 36 % (Fig. 3b); the lower limit of agreement moved from −6.1 % to −11.4 % RH (Fig. 4b). Humidity fell below the 41 % floor of the calibration in 33 % of readings, 438 of the 475 at midday, and there agreement held (bias −1.5 % RH, 90 % of readings within tolerance): extrapolation to drier air cost little, extrapolation to wetter air a great deal. The hour with the largest error was therefore different for each quantity: 12:00–13:00 for temperature (bias 1.26 °C) and 07:00–08:00 for humidity (MAE 5.1 % RH), in each case the hour whose conditions lay furthest from those of the calibration. The late-afternoon window, which matched the calibration conditions, gave the smallest errors for both (temperature RMSE 0.48 °C, humidity RMSE 1.4 % RH).

Illuminance behaved differently. The relative error was smaller above the calibrated range (MAPE 3.7 %, 95 % CI 1.7–6.1) than within it (5.5 %, 4.2–7.1), and the Bland–Altman analysis found no proportional bias in either group (Fig. 4c). Two features of the data account for the difference. First, the absolute error grew far more slowly than the light itself, from a mean of 0.56 klx below 10 klx to 2.8 klx above 60 klx, so the relative error fell with illuminance, from 7.7 % below 10 klx to 3.3–4.0 % above 20 klx. The fall was already complete within the calibrated range (3.3 % at 20–35 klx), so the lower MAPE above the range reflects the light level, not the calibration. Second, the large errors of the extrapolated range came from a single window rather than from the range as a whole. At point 2 at midday on the first day of the 1 min test, in its 12 readings above 64 klx, the sensor read 15.8–18.8 % below the reference, whereas in the 17 readings above 60 klx from the other windows at the same point it read 0.7–3.9 % above it. The BH1750 is linear over its range and its calibration slope was close to 1 (0.95–1.07), so unlike the temperature sensor it gives no reason to expect the relation to change above the calibrated range. The under-reading of that window was proportional rather than capped, which argues against saturation of the sensor (full count at about 55 klx in its default setting, extendable by shortening the measurement time [17]) and is more consistent with a difference in exposure between sensor and reference: the BH1750 faced upwards under the conical cover, whereas the luxmeter was held beside the node at a height that was not recorded, so the two could be shaded differently by the cover, the structure or passing cloud. Shading was not measured, and no field note of shading or cloud was kept for that window. The same exposure difference can arise in any comparison between a mounted sensor and a hand-held reference.

The illuminance measured by the BH1750 is photometric: it weights light by the spectral sensitivity of the human eye, whereas crop growth responds to photosynthetically active radiation (PAR, 400–700 nm) and the greenhouse energy balance to total solar irradiance. The conversion between them depends on the spectrum, which changes with cloud, sun elevation and the cover. In this system the BH1750 serves as a light signal against which a controller switches shading or ventilation; its readings do not convert to PAR, solar irradiance or the light supply of crops without a spectral calibration.

Across points, the error of the temperature sensor rose from the pad end to the fan end of the house (RMSE 0.65, 1.07, and 1.58 °C at points 1, 2 and 3). At midday the reference at points 2 and 3 read 2.3 and 1.9 °C warmer than at point 1 and 6.7 and 3.5 % RH drier, consistent with the air warming and drying after it leaves the evaporative pad. The rise, 0.10 to 0.23 °C m$^{-1}$ of distance from the pad, lies within the 0.06 to 0.27 °C m$^{-1}$ reported along fan-and-pad greenhouses [3, 6, 29]. Excluding the 43 windows whose reference values carry finer resolution than the instrument displays changed the per-point RMSE by at most 0.11 °C and 0.3 % RH and left the ordering of the range classes unchanged: the share of readings within tolerance stayed highest within the calibrated range (80 and 94 %) and lowest above it (39 and 31 %), although below the range it fell to 64 and 80 % for temperature and humidity.

### 3.3 Transmission Interval

Because each interval was run on different days (Section 2.5), the effect of the interval was isolated by subsampling the 1 min series of each window at 5 and 10 min, which compares the intervals on identical weather (Fig. 5). For temperature and humidity the interval hardly mattered. Over the 18 windows, the hourly mean from a 10 min series differed from the 1 min mean by a median of 0.05 °C and 0.15 % RH, and by at most 0.22 °C and 0.91 % RH, about a fifth of the reference accuracy. The hourly maximum was underestimated by at most 0.7 °C and 1.0 % RH. The same asymmetry, means robust to sparse sampling and extremes not, appears in daily temperature records sampled at decreasing frequency [30], and a subsampling test of 1 min temperature and humidity logs in museum rooms found hourly logging sufficient there [31]; a greenhouse changes faster than a museum, and still the 10 min series lost little.

Two qualifications bound these results. First, the subsampled series reproduces what the firmware used here did at the longer intervals: it transmitted one instantaneous reading every 5 or 10 min. A node that averages its readings between transmissions would track the hourly mean at least as well, because averaging smooths fluctuations rather than sampling them by chance, but it would flatten the peaks further, so the losses of maxima reported here are lower bounds for such a node. Second, the 18 windows per quantity cover three times of day on two days at three points in one greenhouse. Within an hour, illuminance varied by 6 to

© 2026 The Authors | CC-BY 4.0

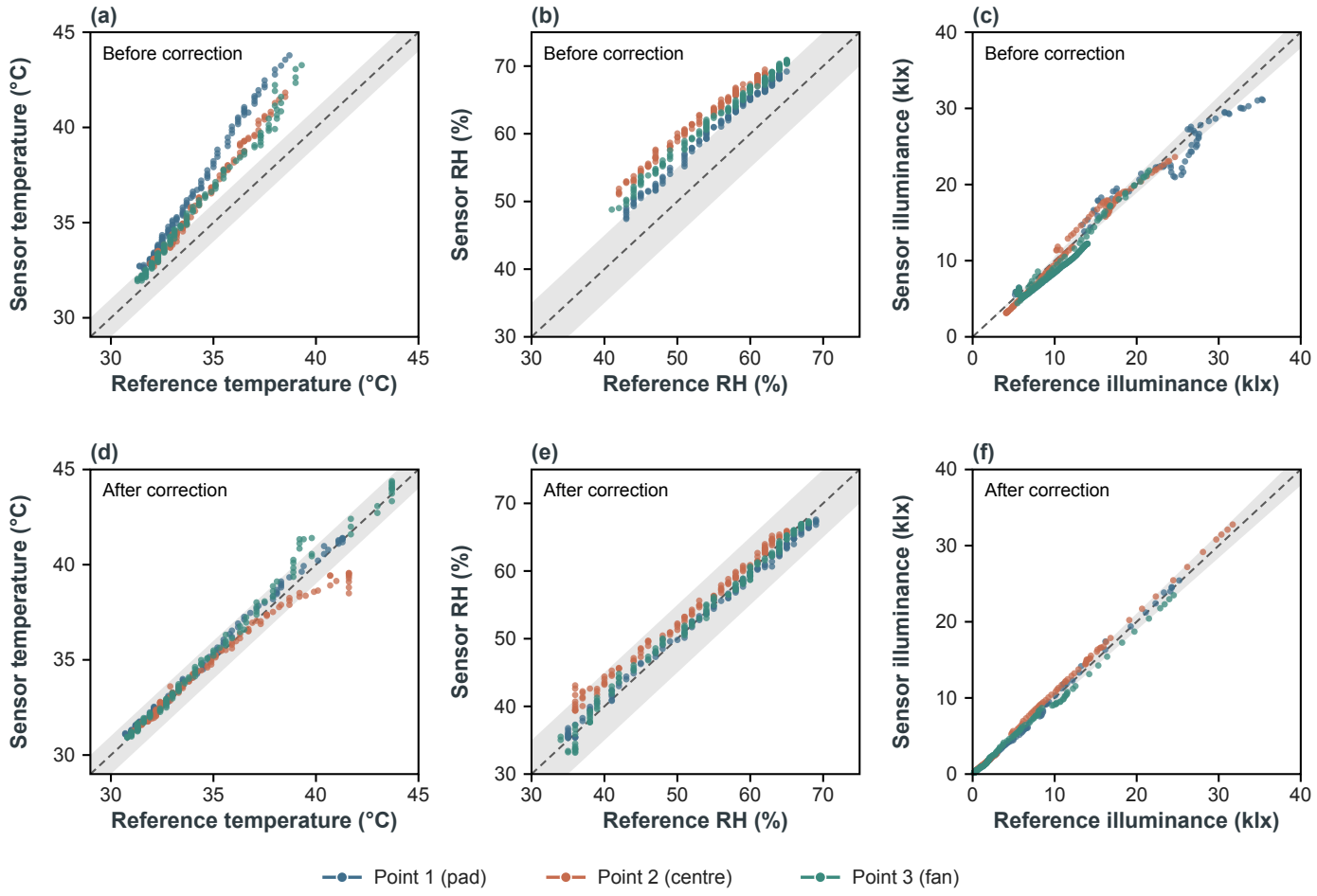



**Figure 2.** Sensor readings against the reference before correction (calibration; a–c) and after correction (validation; d–f): air temperature (a, d), relative humidity (b, e) and illuminance (c, f). Dashed line, 1:1; grey band, stated accuracy of the reference instrument (HTC-2, ±1 °C and ±5 % RH; UT383, ±(4–5 % + digits)). Points 1–3 in colour; 121 readings per point and panel (363 per panel). The calibration (a–c) spanned 31.3–39.3 °C, 41–65 % RH and 4.1–35.4 klx at the reference.

**Table 2.** Agreement between sensor and reference before correction (calibration) and after correction (validation). $a$ and $R^2$, slope and coefficient of determination of Eq. (1); bias and RMSE in the unit of each quantity; MAPE in %. 121 readings per point and stage.

| | Before correction (calibration) | | | | | After correction (validation) | | |
|---|---|---|---|---|---|---|---|---|
| Point | $a$ | $R^2$ | Bias | RMSE | MAPE | Bias | RMSE | MAPE |
| *Air temperature (°C)* | | | | | | | | |
| 1 (pad) | 1.65 | 0.997 | 2.43 | 2.75 | 7.0 | 0.28 | 0.34 | 0.8 |
| 2 (centre) | 1.40 | 0.995 | 1.64 | 1.80 | 4.7 | −0.23 | 0.75 | 1.0 |
| 3 (fan) | 1.34 | 0.991 | 1.51 | 1.73 | 4.3 | 0.34 | 0.54 | 1.0 |
| *Relative humidity (% RH)* | | | | | | | | |
| 1 (pad) | 0.96 | 0.994 | 5.2 | 5.3 | 9.6 | −0.3 | 1.1 | 1.8 |
| 2 (centre) | 0.86 | 0.991 | 8.5 | 8.5 | 16.2 | 2.2 | 2.6 | 4.9 |
| 3 (fan) | 0.90 | 0.995 | 6.7 | 6.7 | 12.3 | 0.1 | 1.1 | 1.8 |
| *Illuminance (*lx*)* | | | | | | | | |
| 1 (pad) | 0.95 | 0.974 | −1 080 | 1 814 | 10.6 | −81 | 296 | 7.1 |
| 2 (centre) | 1.07 | 0.986 | −121 | 839 | 8.8 | 386 | 615 | 6.9 |
| 3 (fan) | 1.04 | 0.975 | −871 | 1 145 | 10.6 | −239 | 487 | 6.0 |

71 klx (median 18 klx), so the windows included both steady light and light varying as under broken cloud, and air temperature reached 47.6 °C. They did not include rain or the operation of shading screens, and the weather of the six days was not recorded; cloud that changes faster or more often than in these hours, or temperatures beyond those observed, could produce larger losses at long intervals.

Illuminance was the exception. Under broken cloud, irradiance at a point can exceed its clear-sky value by more than 50 % on sub-minute time scales [22], and much of the cloud-driven variability lies below one minute [32]. A sparse series samples those changes by chance: the 10 min series shifted the hourly mean by a median of 0.36 klx but by up to 10.1 klx, and missed the hourly maximum by up to 19.9 klx. For a system whose purpose is to trigger shading or ventilation on a light or temperature threshold, a 10 min interval was therefore adequate for hourly means of air temperature and humidity in these windows, with maxima underestimated by up to 0.7 °C, but not for illuminance. The observation guidance of the World Meteorological Organization, which concerns averaged values, treats a 1 min average as the most suitable [21]; a node that sends single readings, as here, has no averaging to smooth the light signal. The result also fits the time scale on which greenhouse climate is controlled, of the order of minutes [33].

### 3.4 Implications for Low-Cost Greenhouse Monitoring

Within the conditions they were calibrated in, the corrected sensors agreed with the reference to within its stated accuracy; above those conditions they did measurably worse. The practical consequence concerns

© 2026 The Authors | CC-BY 4.0

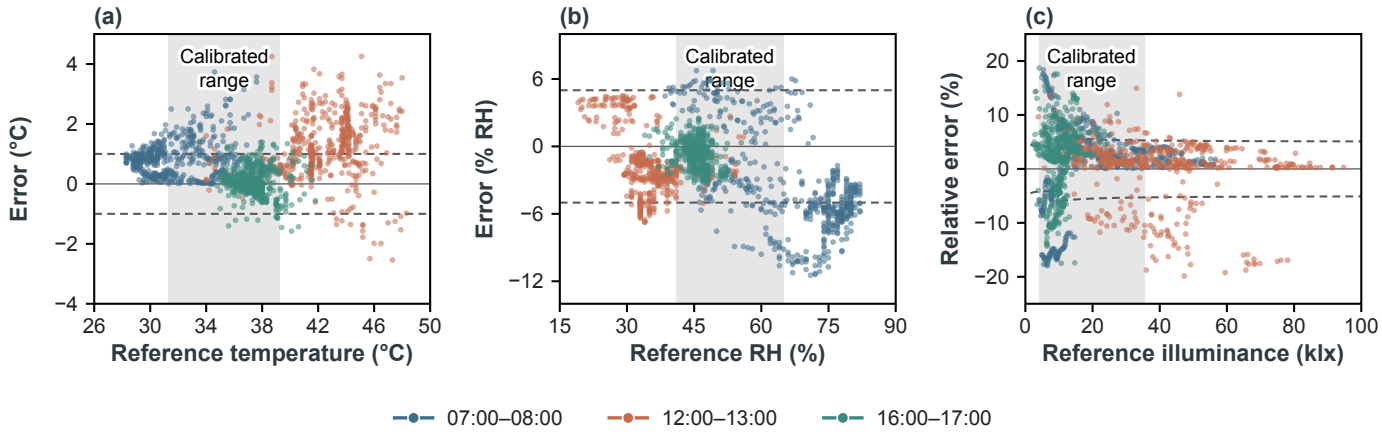



**Figure 3.** Error of the corrected sensors in the performance tests against the reference value: air temperature (a), relative humidity (b) and illuminance (c, relative error). Error = corrected sensor reading − reference reading. Grey band, range covered by the calibration (31.3–39.3 °C, 41–65 % RH, 4.1–35.4 klx); dashed lines, stated accuracy of the reference (±1 °C, ±5 % RH, ±(4–5 % + digits) for illuminance). Colour, hourly window. 1458 readings per panel (3 points × 486), all three transmission intervals pooled.

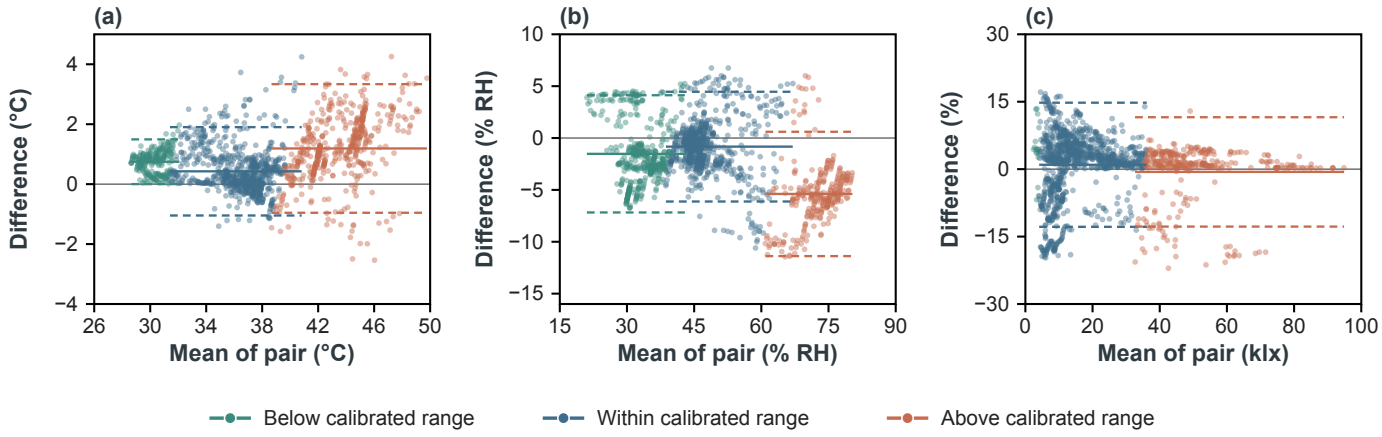



**Figure 4.** Bland–Altman plots of the corrected sensors in the performance tests: air temperature (a), relative humidity (b) and illuminance (c, difference relative to the pair mean). Difference = corrected sensor reading − reference reading. Colour, position of the reference value relative to the calibrated range; solid line, mean difference; dashed lines, 95 % limits of agreement, each drawn over the extent of its group. Readings below, within and above the range: 233, 746 and 479 (a); 475, 703 and 280 (b); 18, 1089 and 351 (c; no limits drawn for the 18 readings below the range).

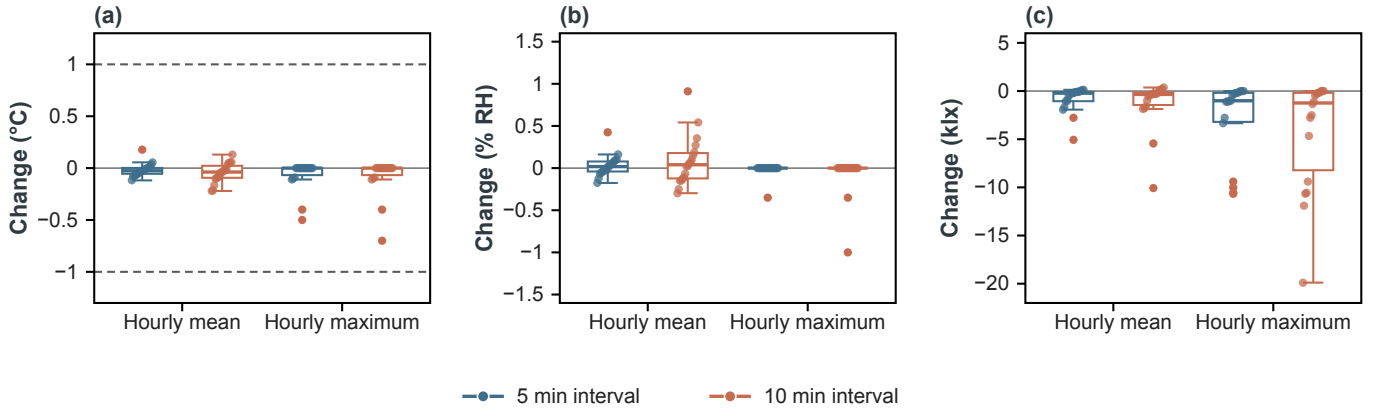



**Figure 5.** Change in the hourly mean and hourly maximum when the 1 min series is subsampled at 5 and 10 min: air temperature (a), relative humidity (b) and illuminance (c). Change = statistic of the subsampled series (13 or 7 readings) − statistic of the full 1 min series (61 readings), for the reference readings. Each dot is one hourly window; 18 windows per panel (3 points × 3 windows × 2 days). Dashed lines in (a), stated accuracy of the reference (±1 °C).

the calibration window. A two-hour calibration in the late afternoon covered 31–39 °C and 41–65 % RH, whereas the house spanned 28–48 °C and 19–82 % RH in the performance tests. A calibration that spans a full diurnal cycle, or at least includes a midday and an early-morning hour, would cover the conditions in which a controller acts and should remove most of the extrapolation error seen here, provided the fitted form follows the relation between sensor and reference over the wider range, which may need a non-linear term at high temperature; this implication was not tested here. Similar advice comes from a systematic review of low-cost temperature sensors found that the temperature range covered changes the calibration outcome and called for calibration steps across the range of use [10], and a laboratory evaluation of seven low-cost thermohygrom-

© 2026 The Authors | CC-BY 4.0

**Table 3.** Agreement between corrected sensors and reference in the performance tests, by measurement point and by position of the reference value relative to the range covered by the calibration (31.3–39.3 °C, 41–65 % RH and 4.1–35.4 klx). $n$, reading pairs, all three transmission intervals pooled. Bias, MAE and RMSE in the unit of each quantity; MAPE in %; $a$ and $R^2$, slope and coefficient of determination of corrected reading on reference. Bootstrap confidence intervals in the text.

| Subset | $n$ | Bias | MAE | RMSE | MAPE | $a$ | $R^2$ |
|---|---|---|---|---|---|---|---|
| *Air temperature (°C)* | | | | | | | |
| Point 1 (pad) | 486 | 0.38 | 0.49 | 0.65 | 1.3 | 1.02 | 0.985 |
| Point 2 (centre) | 486 | 0.59 | 0.85 | 1.07 | 2.3 | 0.99 | 0.970 |
| Point 3 (fan) | 486 | 1.22 | 1.28 | 1.58 | 3.3 | 1.08 | 0.972 |
| Below range | 233 | 0.75 | 0.75 | 0.84 | 2.5 | 0.98 | 0.809 |
| Within range | 746 | 0.43 | 0.58 | 0.86 | 1.6 | 0.86 | 0.853 |
| Above range | 479 | 1.19 | 1.39 | 1.62 | 3.2 | 1.10 | 0.817 |
| *Relative humidity (% RH)* | | | | | | | |
| Point 1 (pad) | 486 | −2.8 | 3.4 | 4.3 | 6.3 | 0.90 | 0.958 |
| Point 2 (centre) | 486 | −0.6 | 3.3 | 4.0 | 7.9 | 0.91 | 0.930 |
| Point 3 (fan) | 486 | −2.4 | 2.5 | 3.1 | 4.9 | 0.90 | 0.988 |
| Below range | 475 | −1.5 | 2.9 | 3.3 | 8.8 | 0.69 | 0.576 |
| Within range | 703 | −0.8 | 2.1 | 2.8 | 4.1 | 0.88 | 0.786 |
| Above range | 280 | −5.4 | 5.8 | 6.2 | 7.8 | 0.97 | 0.651 |
| *Illuminance (*lx*)* | | | | | | | |
| Point 1 (pad) | 486 | 291 | 596 | 804 | 4.3 | 1.01 | 0.996 |
| Point 2 (centre) | 486 | −579 | 1 663 | 2 733 | 7.4 | 0.96 | 0.980 |
| Point 3 (fan) | 486 | 664 | 664 | 874 | 3.7 | 1.01 | 0.999 |
| Below range | 18 | 145 | 214 | 245 | 6.4 | 0.88 | 0.819 |
| Within range | 1089 | 254 | 713 | 913 | 5.5 | 1.02 | 0.990 |
| Above range | 351 | −273 | 1 824 | 3 115 | 3.7 | 0.98 | 0.946 |

eters advised fixing the calibration range to that of the intended study [19]. Most such calibrations, however, are made indoors or under controlled conditions [10], and a field correction trained at one site degraded when applied where conditions differed [14]. The present data put a size on the consequence inside a working greenhouse: agreement within the reference accuracy fell from 83 to 38 % of temperature readings once the air rose above the calibrated range.

The findings come from one greenhouse, three nodes and one pair of sensor models, compared with reference instruments of limited accuracy that are not traceable, on days whose dates, weather and cooling operation were not recorded. They show what happens to a field calibration of this kind when the conditions leave its range; they do not establish that the same errors, or the same intervals, apply to other tropical greenhouses, other cooling regimes or other sensors. Transfer to another house is most plausible where the same mechanism applies: a low-cost node calibrated in a short window and then used across a wider diurnal range of temperature and humidity.

## 4. CONCLUSIONS

Three low-cost nodes (ESP32 with SHT20 and BH1750 sensors) were calibrated against reference instruments in a fan-and-pad cooled greenhouse in the humid tropics and followed through 1458 paired readings per quantity at three times of day. A two-hour late-afternoon calibration reduced temperature and humidity offsets of up to 2.4 °C and 8.5 % RH to at most 0.34 °C and 2.2 % RH in validation, and within the conditions it covered the corrected sensors agreed with the reference to within its stated accuracy: 83 % of temperature readings and 92 % of humidity readings fell inside ±1 °C and ±5 % RH. Because the reference instruments were not traceable, this is agreement with them, not established accuracy. Above those conditions the agreement failed, with 38 % of readings within tolerance above 39.3 °C, mostly at midday, and 36 % above 65 % RH in the morning, and the temperature difference grew with temperature only beyond the fitted range, where the sensor–reference relation steepened and the linear correction could not follow. The late-afternoon window, the one that matched the calibration, gave the smallest errors, a temperature RMSE of 0.48 °C and a humidity RMSE of 1.4 % RH. Subsampling showed that, in the 18 hourly windows tested, a 10 min interval changed hourly means of temperature and humidity by at most 0.22 °C and 0.91 % RH but missed hourly peaks of illuminance by up to 19.9 klx; these figures describe the conditions sampled and may not hold under faster-changing weather. For low-cost nodes in this greenhouse, most of the disagreement on which cooling decisions rest arose outside the calibration window. Whether a calibration spanning a full diurnal cycle, with the sensors in ventilated radiation shields and referenced to an aspirated, traceable instrument, removes the extrapolation error, and whether the pattern holds in other greenhouses and with other sensors, remains to be tested.

## CRediT AUTHORSHIP CONTRIBUTION STATEMENT

**Zunanik Mufidah:** Conceptualization, Methodology, Formal analysis, Visualization, Supervision, Resources, Writing – original draft, Writing – review & editing. **Mahardika Priya Tumanggor:** Investigation, Data curation, Software. **Kisna Pertiwi:** Supervision, Writing – review & editing.

## DECLARATION OF COMPETING INTEREST

The authors declare that they have no known competing financial interests or personal relationships that could have appeared to influence the work reported in this paper.

## DATA AVAILABILITY

The data supporting the findings of this study are available from the corresponding author on reasonable request.

## FUNDING

This research received no external funding.

## REFERENCES

[1] B. Rabbi, Z.-H. Chen, S. Sethuvenkatraman, Protected cropping in warm climates: A review of humidity control and cooling methods, Energies 12 (2019) 2737. doi:10.3390/en12142737.

[2] I. Impron, S. Hemming, G. Bot, Simple greenhouse climate model as a design tool for greenhouses in tropical lowland, Biosystems Engineering 98 (2007) 79–89. doi:10.1016/j.biosystemseng.2007.03.028.

[3] X. Wei, B. Li, H. Lu, J. Guo, Z. Dong, F. Yang, E. Lü, Y. Liu, Distribution characteristics and prediction of temperature and relative humidity in a south china greenhouse, Agronomy 14 (2024) 1580. doi:10.3390/agronomy14071580.

[4] R. Shamshiri, Measuring optimality degrees of microclimate parameters in protected cultivation of tomato under tropical climate condition, Measurement 106 (2017) 236–244. doi:10.1016/j.measurement.2017.02.028.

[5] I. M. Al-Helal, Effects of ventilation rate on the environment of a fan-pad evaporatively cooled, shaded greenhouse in extreme arid climates, Applied Engineering in Agriculture 23 (2007) 221–230. doi:10.13031/2013.22605.

[6] A. López, D. L. Valera, F. D. Molina-Aiz, A. Peña, Sonic anemometry to evaluate airflow characteristics and temperature distribution in empty mediterranean greenhouses equipped with pad–fan and fog systems, Biosystems Engineering 113 (2012) 334–350. doi:10.1016/j.biosystemseng.2012.09.006.

© 2026 The Authors | CC-BY 4.0

[7] N. Chamara, M. D. Islam, G. F. Bai, Y. Shi, Y. Ge, Ag-iot for crop and environment monitoring: Past, present, and future, Agricultural Systems 203 (2022) 103497. doi:10.1016/j.agsy.2022.103497.

[8] T. Pisanu, S. Garau, P. Ortu, L. Schirru, C. Macciò, Prototype of a low-cost electronic platform for real time greenhouse environment monitoring: An agriculture 4.0 perspective, Electronics 9 (2020) 726. doi:10.3390/electronics9050726.

[9] E. D. Wardihani, E. U. Sari, Helmy, A. S. Nugroho, Y. Badruzzaman, A. Nursyahid, T. A. Setyawan, M. F. I. Nugraha, Pemantauan dan pengendalian parameter greenhouse berbasis IoT dengan protokol MQTT, Jurnal Nasional Teknik Elektro dan Teknologi Informasi 13 (2024) 38–43. doi:10.22146/jnteti.v13i1.8564.

[10] J. A. Abdinoor, Z. K. Hashim, B. Horváth, S. Zsebő, D. Stencinger, G. Hegedüs, L. Bede, A. Ijaz, I. M. Kulmány, Performance of low-cost air temperature sensors and applied calibration techniques—a systematic review, Atmosphere 16 (2025) 842. doi:10.3390/atmos16070842.

[11] T. Araújo, L. Silva, A. Moreira, Evaluation of low-cost sensors for weather and carbon dioxide monitoring in internet of things context, IoT 1 (2020) 286–308. doi:10.3390/iot1020017.

[12] A. J. Terando, E. Youngsteadt, E. K. Meineke, S. G. Prado, Ad hoc instrumentation methods in ecological studies produce highly biased temperature measurements, Ecology and Evolution 7 (2017) 9890–9904. doi:10.1002/ece3.3499.

[13] J. M. Tarara, G.-A. Hoheisel, Low-cost shielding to minimize radiation errors of temperature sensors in the field, HortScience 42 (2007) 1372–1379. doi:10.21273/HORTSCI.42.6.1372.

[14] K. Yamamoto, T. Togami, N. Yamaguchi, S. Ninomiya, Machine learning-based calibration of low-cost air temperature sensors using environmental data, Sensors 17 (2017) 1290. doi:10.3390/s17061290.

[15] S. A. Bell, P. A. Carroll, S. L. Beardmore, C. England, N. Mander, A methodology for study of in-service drift of meteorological humidity sensors, Metrologia 54 (2017) S63–S73. doi:10.1088/1681-7575/aa6dd0.

[16] Sensirion AG, Staefa, Switzerland, Datasheet SHT20: Humidity and Temperature Sensor IC, Version 5 (Oct. 2022).
URL https://sensirion.com/media/documents/CCDE1377/635000A2/Sensirion_Datasheet_Humidity_Sensor_SHT20.pdf

[17] ROHM Co., Ltd., Kyoto, Japan, BH1750FVI: Digital 16bit Serial Output Type Ambient Light Sensor IC, Technical Note No.11046EDT01, Rev.D (Nov. 2011).
URL https://www.mouser.com/datasheet/2/348/bh1750fvi-e-186247.pdf

[18] J. A. Nava-Pintor, U. E. Alcalá-Rodríguez, H. A. Guerrero-Osuna, M. E. Mata-Romero, E. Lopez-Neri, F. García-Vázquez, L. O. Solís-Sánchez, R. Carrasco-Navarro, L. F. Luque-Vega, Development and evaluation of solar radiation sensor using cost-effective light sensors and machine learning techniques, Technologies 13 (2025) 182. doi:10.3390/technologies13050182.

[19] F. Salamone, G. Chinazzo, L. Danza, C. Miller, S. Sibilio, M. Masullo, Low-cost thermohygrometers to assess thermal comfort in the built environment: A laboratory evaluation of their measurement performance, Buildings 12 (2022) 579. doi:10.3390/buildings12050579.

[20] X. Sun, S. Yan, B. Wang, L. Xia, Q. Liu, H. Zhang, Air temperature error correction based on solar radiation in an economical meteorological wireless sensor network, Sensors 15 (2015) 18114–18139. doi:10.3390/s150818114.

[21] World Meteorological Organization, Geneva, Guide to Instruments and Methods of Observation, Volume I: Measurement of Meteorological Variables (2023).
URL https://library.wmo.int/records/item/68695-guide-to-instruments-and-methods-of-observation

[22] G. M. Lohmann, Irradiance variability quantification and small-scale averaging in space and time: A short review, Atmosphere 9 (2018) 264. doi:10.3390/atmos9070264.

[23] Uni-Trend Technology (China) Co., Ltd., Dongguan, China, UT383 Mini Light Meters: Operating Instruction (2016).
URL https://meters.uni-trend.com/download/ut383-user-manual/

[24] Generic manufacturer (vendor specification sheet), HTC-2 Digital Thermometer Hygrometer: Product Specification (vendor sheet) (2022).
URL https://5.imimg.com/data5/SELLER/Doc/2022/11/NB/UK/VK/25615324/hygrometer.pdf

[25] H. R. Künsch, The jackknife and the bootstrap for general stationary observations, The Annals of Statistics 17 (3) (1989) 1217–1241. doi:10.1214/aos/1176347265.

[26] J. M. Bland, D. G. Altman, Statistical methods for assessing agreement between two methods of clinical measurement, The Lancet 327 (8476) (1986) 307–310. doi:10.1016/S0140-6736(86)90837-8.

[27] O. A. Alduchov, R. E. Eskridge, Improved Magnus form approximation of saturation vapor pressure, Journal of Applied Meteorology 35 (1996) 601–609. doi:10.1175/1520-0450(1996)035<0601:IMFAOS>2.0.CO;2.

[28] H. Vömel, H. Selkirk, L. Miloshevich, J. Valverde-Canossa, J. Valdés, E. Kyrö, R. Kivi, W. Stolz, G. Peng, J. A. Diaz, Radiation dry bias of the Vaisala RS92 humidity sensor, Journal of Atmospheric and Oceanic Technology 24 (2007) 953–963. doi:10.1175/JTECH2019.1.

[29] C. Kittas, T. Bartzanas, A. Jaffrin, Temperature gradients in a partially shaded large greenhouse equipped with evaporative cooling pads, Biosystems Engineering 85 (2003) 87–94. doi:10.1016/S1537-5110(03)00018-7.

[30] W. A. Gough, A. Žaknić-Ćatović, A. Zajch, Sampling frequency of climate data for the determination of daily temperature and daily temperature extrema, International Journal of Climatology 40 (2020) 5451–5463. doi:10.1002/joc.6528.

[31] F.-J. García-Diego, E. Verticchio, P. Beltrán, A. Siani, Assessment of the minimum sampling frequency to avoid measurement redundancy in microclimate field surveys in museum buildings, Sensors 16 (2016) 1291. doi:10.3390/s16081291.

[32] W. B. Mol, W. H. Knap, C. C. van Heerwaarden, Ten years of 1 Hz solar irradiance observations at Cabauw, the Netherlands, with cloud observations, variability classifications, and statistics, Earth System Science Data 15 (2023) 2139–2151. doi:10.5194/essd-15-2139-2023.

[33] E. J. van Henten, Greenhouse climate management: An optimal control approach, Ph.D. thesis, Wageningen Agricultural University, Wageningen, The Netherlands (1994). doi:10.18174/205106.

© 2026 The Authors | CC-BY 4.0